



A new approach for secure communication in industrial automation based on new finite-time chaotic synchronization scheme

Mehdi Golshani Amin¹, Javad Mostafaei^{1*}

¹ Faculty of Electrical Engineering, University of Ghiaseddin Jamshid Kashani, Abyek, Qazvin, Iran.

Received: 13-Apr-2022, Revised: 17-May-2022, Accepted: 19-May-2022.

Abstract

This paper constructs a novel 4D system with nonlinear complex dynamic behaviors. By analyzing the hyperchaotic attractors, bifurcation diagram, equilibrium points, Poincare map, Kaplan–Yorke dimension, and Lyapunov exponent behaviors, we prove that the introduced system has complex and nonlinear behavior. Next, the work describes a finite-time terminal sliding mode controller scheme for the synchronization and stability of the novel hyperchaotic system. All the results obtained from the proposed control are verified using Lyapunov stability theory. For synchronization, both systems designed with different parameters and model uncertainties are disturbed. Both stages of the finite-time terminal sliding mode controller have been shown to have fast convergence properties. Simply put, it has been shown that the state paths of both master and slave systems can reach each other in a finite–time. The new controller feature is that the terminal sliding surface designed with a high–order power function of error and derivative of error, is stable in finite–time. At last, using the MATLAB simulation, the results are confirmed for the new hyperchaotic system.

Keywords: Hyperchaotic System, Chaotic Analysis, Fast Synchronization, Finite-Time Terminal Sliding Mode Control.

1. INTRODUCTION

In the current digital age, we have witnessed an increasing trend towards secure communication links with the aim of trading

transactions, online shopping, and banking. Certainly, these wide applications of secure communications will increase exponentially in the future. One of the challenges in this area is to keep information secure and increase the security of data transmission networks [1]. One of the areas in which

*Corresponding Authors Email:
javadmstafaei1982@gmail.com

communication technologies are being developed today is the transfer of information to industrial applications, especially industrial automation [2-4]. Due to the importance of information in this area, the transfer of information in the usual networks will present risks such as easy access to information. Therefore, one of the necessities of information transfer, especially Industrial information, is to increase the security of information transfer [5, 6]. One way to increase security in the transmission of industrial information is to encrypt information using chaotic functions [7].

Chaotic and hyperchaotic systems have a number of intrinsic properties including high oscillations as well as complex nonlinear dynamical equations [8, 9]. Two very important features of these systems are the uncertainties in the system parameters and the extreme sensitivity to very small changes in their initial conditions. Chaos programs and methods of analysis were developed over time. Given that chaotic systems are unpredictable, this very important feature can be used in many fields such as image encryption [10], robotic [11], biological networks [12], neuroscience [13], secure communication [14], and information processing [15]. The research on chaotic systems has achieved considerable progress. Many new 3D chaotic systems were accepted, in which the Chen [16], Lu [17] and Qi [18] systems are generic. These chaotic systems because they are simple in structure and have only one Lyapunov exponent, faults of feeble security allow them to be easily cracked. Hence, Rossler created the first hyperchaotic system and determined it as a system with two or more Lyapunov

exponents [19]. An important difference between chaotic and hyperchaotic systems is that high-order hyperchaotic systems have more complex behavior and higher volatility [20, 21]. To create a hyperchaotic system, it is necessary to increase the system dimension, however, this may lead to instability. In a chaotic secure communication system, to ensure secure message transmission, similar systems must be used on both sides of the master and the slave. In order to have a complete and successful transmission, chaotic systems in the master-slave configuration must be synchronized. Dynamic synchronization of these systems is a very important phenomenon [22], which has been displayed in many scientific structures [23]. Synchronization of chaotic systems is one of the main control approaches that has been considered for many years. For synchronization, an appropriate control technique is used to move the systems of the master to the slave. In recent years, many controllers have been used to synchronize hyperchaotic systems [24-28]. Since time plays a basic role in the transmission of industrial information, therefore, the transmission of information in the fastest time is crucial. Between the stated methods, sliding mode control (SMC) has some special specs such as parametric uncertainties, robustness versus, simply implement, suitable transient response, reduce the order of the system, less sensitivity to bounded disturbance, and computational simplicity [29]. Over several years much research has been devoted to the development and application of SMC design [30-33].

Although SMC is very popular and efficient, but this method has a big drawback called chattering. In practice, chattering is a very undesirable phenomenon because it can increase energy consumption, cause mechanical wear in systems and actuators and deteriorate controller performance. So, in designing the controller we will have two goals, eliminating the chattering phenomenon and controlling the function as quickly as possible. A lot of research has been done to solve these problems. The application of a new chattering-free sliding mode control technique with both-differential and integral operators for synchronizing and controlling nonlinear disturbance systems with unknown parameters is stated in [34]. Utilization of a new PID sliding mode control to eliminate the effect of chattering phenomenon as well as to achieve optimal state-of-the-art in finite time and high accuracy and to use estimation theory to adjust the parameters with regard to consistent disturbances in the system is stated in [35].

Employing new powerful controllers for finite-time as well as eliminating deleterious effects on the system is studied in [36, 37]. The new controllers are developed for secure communication of two various chaotic systems with unknown parameters, external disturbances, and systemic uncertainty, by combining adaptive back-stepping in a finite-time terminal sliding mode control (FTSMC) studies. The FTSMC supplies faster convergence and more precise control than the conventional SMC. The FTSMC method accomplishes both robustness against uncertainties and external disturbances and guarantees system stability in a finite-time.

However, some engineering problems are expected to reach synchronization within a finite-time. The fast synchronization has many advantages, such as optimality of convergence time, disturbance rejection properties and better robustness.

Decoding an unauthorized receiver without knowing the initial conditions and dynamics of a hard-working system is difficult. One of the ways to increase security in chaotic communications is to use the high-order dimensional dynamics, because high-order dynamic regeneration and discovery of messages for unauthorized recipients using difficult timescale reduction methods are difficult. Other ways to increase security in chaotic secure communications can point out the complexity of the systems dynamics, because the more complex the structure of the system and its more parameters, the more difficult system decoding. The design of high-order chaotic and hyperchaotic systems as well as the analysis of their intrinsic properties and the stability analysis of these systems are some of the research that has been done in this field [38-40]. Asymptotic stability is a weaker concept than finite-time stability. In finite-time stability, system state variables converge to their equilibrium point more rapidly in a finite-time. The term "terminal" refers to the meaning of finite-time stability. Depending on the structure of the systems, there are many applications that need to be stable in a finite-time. The paper consists of the following main contributions:

- I. Design of an exponential 4D hyperchaotic system, analysis, and acquisition of its inherent properties.

- II. The introduction of a new controller based on FTSMC for the fast synchronization of two different hyperchaotic systems.
- III. Eliminating the destructive chattering phenomenon by introducing a new sliding surface.

The structure of the rest of this article is as follows: Section 2 provides the dynamic model of the hyperchaotic system and its benefits and features. In the following, the fast synchronization problem of hyperchaotic systems in finite-time is formulated. Section 3 is used to describe the structure of the FTSMC and analyze the stability and finite-time convergence of the desired system. In Section 4, numerical simulations are performed to prove the methods. Section 5 contains some conclusions from the previous sections.

2. PROBLEM DESCRIPTION AND PRELIMINARIES

2.1. Model of Hyperchaotic System

The dynamics of the new 4D system are described as:

$$\begin{aligned}
 \dot{x}_1(\tau) &= a_1(x_2 - x_1) - a_2x_4 \\
 &\quad - a_3x_3^2 - a_4x_2x_3 \\
 \dot{x}_2(\tau) &= a_5x_2 + a_6x_4 - a_1x_1^2 \\
 &\quad - a_7x_2x_3 - a_8x_1x_2 - a_9x_1x_2x_3 \\
 \dot{x}_3(\tau) &= -a_2x_3 + a_{10}x_1^2 + x_1x_2x_3 \\
 \dot{x}_4(\tau) &= -a_{11}x_1 + a_9x_3 + a_7x_1x_2x_3 \\
 &\quad + a_8x_1x_2 + a_{10}x_2x_3x_4 + a_{12}x_1x_3x_4
 \end{aligned} \quad (1)$$

where $x_i, (i=1, \dots, 4)$ and $a_i, (i=1, \dots, 12)$ are the state variables and constant positive

parameters of the system (1). With $a_1 = 15, a_2 = 4, a_3 = 15, a_4 = 8.5, a_5 = 0.12, a_6 = 21.2, a_7 = 11, a_8 = 3.5, a_9 = 8, a_{10} = 5, a_{11} = 13, a_{12} = 20.1$, system (1) exhibits complex hyperchaotic behavior.

2.2. Basic Properties and Dynamic Behaviors of Hyperchaotic System

This section gives the natural properties of the new hyperchaotic system such as chaotic attractors, equilibrium points, Kaplan–Yorke dimension, eigenvalues, Lyapunov exponents, Poincare map, and bifurcation diagram.

2.2.1. Equilibrium Points and Eigenvalues Analysis

By setting the differential equations in (1) to zero, one of the equilibrium points is the origin. When the parameter values are considered as in (1), the system linearization matrix [41] at the zero equilibrium point is given by

$$J = \left. \frac{\partial F_i}{\partial x_j}(x) \right|_{Q^*} = \begin{bmatrix} -a_1 & a_1 & 0 & -a_2 \\ 0 & a_5 & -a_9 & a_6 \\ -a_1 & -a_1 & -a_2 & -a_1 \\ -a_{11} + a_{12} & a_{12} & a_9 + a_{12} & a_{12} \end{bmatrix} \quad (2)$$

According to (2), the system eigenvalues are found as follows:

$p(s) = |sI_d - J| = 0$ with, I_d was an 4×4 identity matrix. That is,

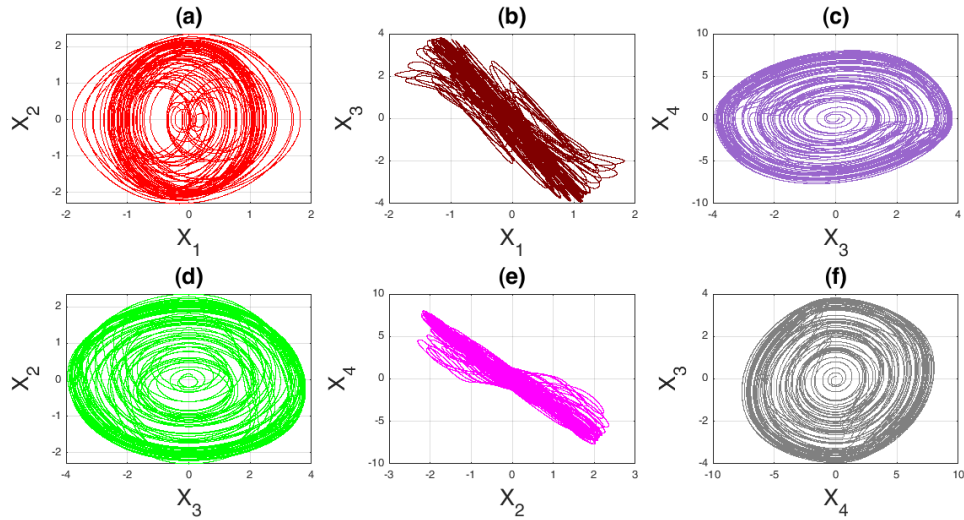


Fig. 1. $x - y$ plan of the system (1).

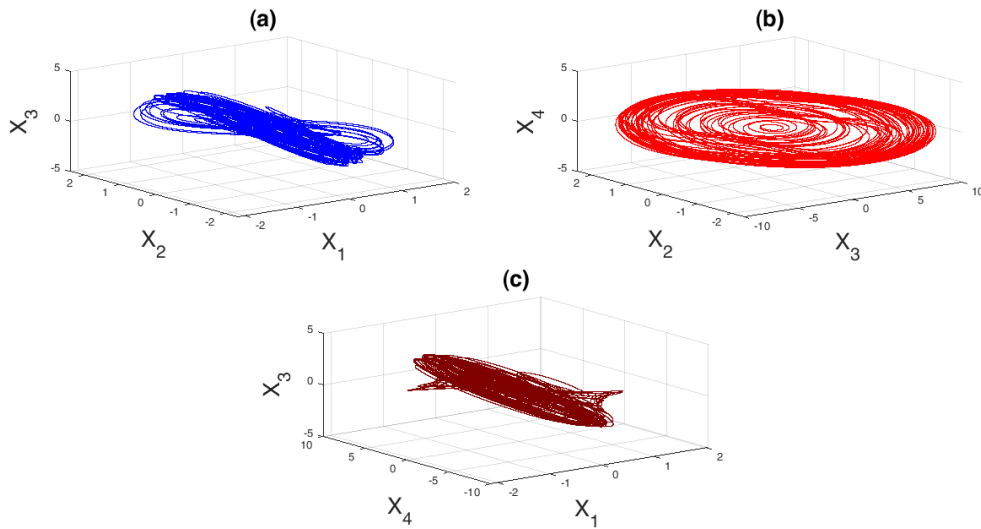


Fig. 2. $x - y - z$ plan of the system (1).

$$[\Delta(s) = s^4 + A_1s^3 + A_2s^2 + A_3s + A_4]$$

$$A_1 = (a_1 + a_2 - a_5 - a_{12})$$

$$A_2 = (-a_6a_{12} - a_1a_5 + a_1a_2 - a_2a_5 - a_1a_{12} + a_5a_{12} - a_2a_{12} + a_2a_5a_{12}) \quad (3)$$

$$A_3 = (-a_1a_6a_{12} - a_2a_6a_{12} - a_1a_2a_5 + a_1a_5a_{12} - a_1a_2a_{12})$$

$$A_4 = (a_1a_2a_6a_{12} + a_1a_2a_5a_{12} - a_1a_2a_9a_{11} + a_1a_2a_9a_{12} - a_1^2a_9a_{11} + a_1^2a_9a_{12})$$

Using parameter values in (1), the eigenvalues are $s_{1,2} = -19.5624 \pm 13.3435j$,

$s_{3,4} = 19.7649 \pm 12.1173j$. Thus, the origin is an unstable saddle.

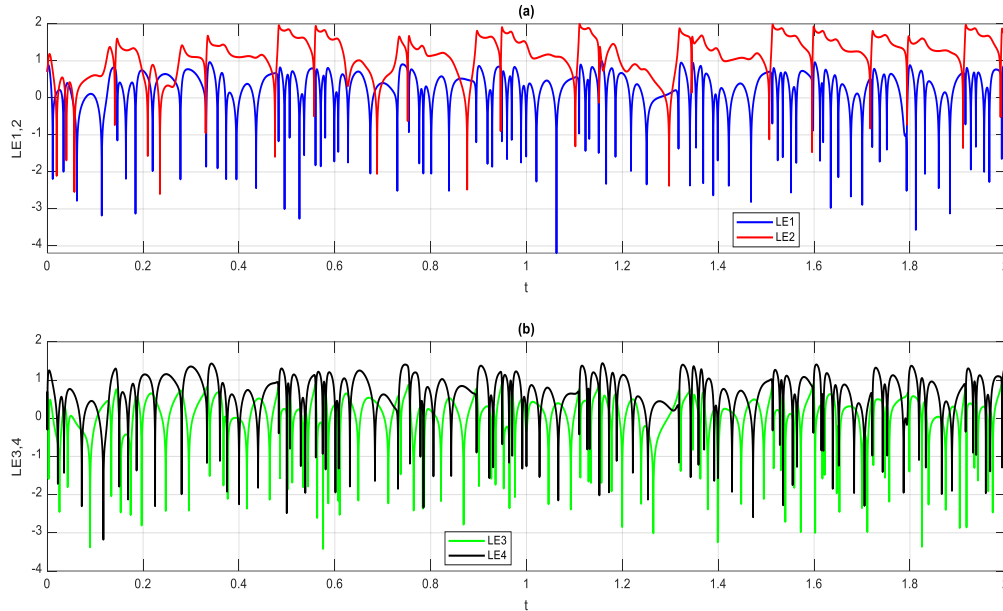


Fig. 3. LEs of the system (1) in (a) LE1, LE2 and (b) LE3, LE4.

2.2.2. Chaotic Attractors Analysis

The system (1) divergence is as follows:

$$\begin{aligned} \nabla V &= \sum_{i=1}^4 \frac{\partial \dot{x}_i}{\partial x_i} \\ &= -a_1 + a_5 - a_9 - a_2 + a_{12} \\ &= 15 + 0.12 - 8 - 4 + 19.75 \\ &= 20.1 > 0 \end{aligned} \quad (4)$$

The convergence speed of the system (1) to its attractor is $e^{-(a_1 + a_5 - a_9 - a_2 + a_{12})\tau}$. So, as time goes on to the infinite, system (1) is constrained and settles on an attractor [42]. the phase portrait diagrams of the system (1) are shown in Fig. 1 and Fig. 2.

2.2.3. Lyapunov Exponents and Kaplan-York Dimension

Divergence and convergence of states of a nonlinear system are determined by its

Lyapunov exponents (LEs) representation. If Lyapunov exponents are positive, it indicates the chaotic behavior of the system [43, 44]. A system is hyperchaotic if there are two or more than two positive LEs. The LEs of the exponential hyperchaotic system (1) with different initial conditions $(x_1(\tau_0) = 2)$, $(x_2(\tau_0) = 7)$, $(x_3(\tau_0) = 7.2)$, $(x_4(\tau_0) = -1.1)$, are numerically found as $LE_1 = 0.132$, $LE_2 = 0.035$, $LE_3 = 0$, $LE_4 = -1.250$, shown in Fig. 3. For these values of Lyapunov exponents, the Kaplan–York dimension [45] of the 4D hyperchaotic designed system, is defined as:

$$\begin{aligned} D_{KY} &= t + \frac{\sum_{i=1}^t LE_i}{|LE_{t+1}|} \\ &= 3 + \frac{LE_1 + LE_2 + LE_4}{|LE_3|} = 3.13 \end{aligned} \quad (5)$$

which is fractional.

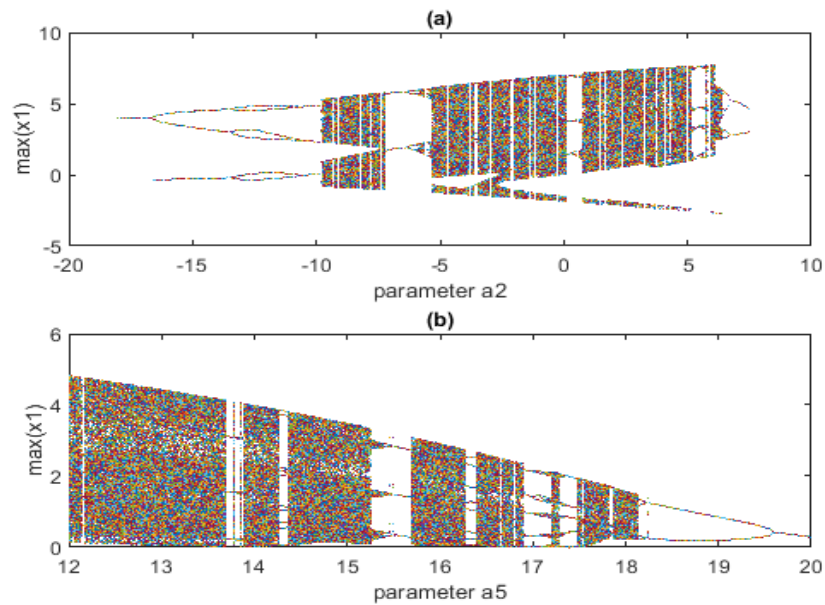


Fig. 4. Bifurcation diagrams of the system (1) in: (a) (a_2, x_1) , $a_2 \in (-20, 10)$ and (b) (a_5, x_1) , $a_5 \in (12, 20)$.

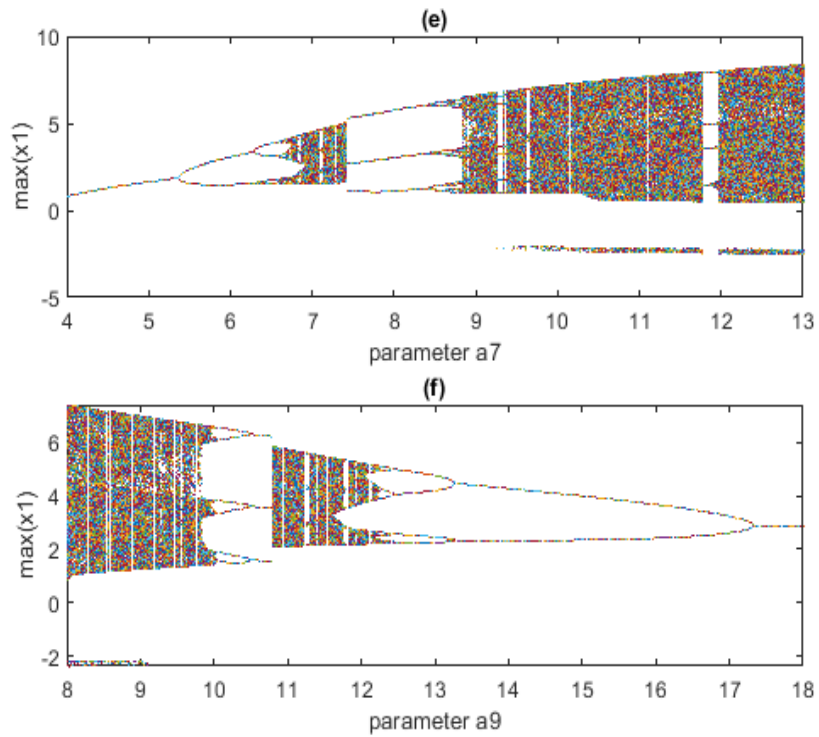


Fig. 5. Bifurcation diagrams of the system (1) in: (e) (a_7, x_1) , $a_7 \in (4, 13)$ and (f) (a_9, x_1) , $a_9 \in (8, 18)$.

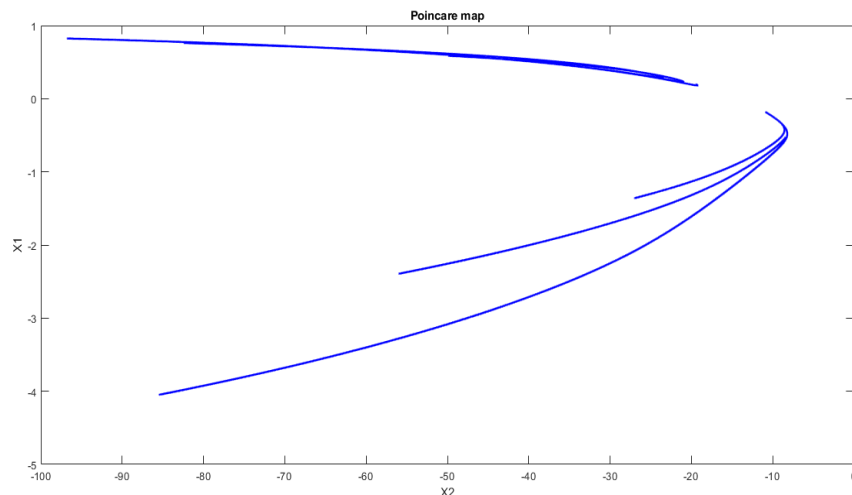


Fig. 6. Poincaré map of the system (1) in $x_1 - x_2$ plan.

2.2.4. Bifurcation Diagram Analysis

To investigate the dependence of the parameters of the new exponential hyperchaotic system (1), we need to draw and analyze the bifurcation diagram. In Fig. 4 and Fig. 5 bifurcation diagrams of the system (1) are plotted. The system enters into chaotic oscillations with routine period doubling. Bifurcation diagrams show the behavior of a system with respect to changes in the system parameter and provide an explanation of the system's absorbent behavior [46, 47].

2.2.5. Poincaré Map Analysis

As an interesting method, we use the Poincaré map to describe the folding attributes of the chaotic system. To study the performance and behavior of continuous dynamical systems, similar the proposed

system (1), we can use the Poincaré map, one of the most popular topics in nonlinear dynamic analysis. Fig. 6 shows the Poincaré maps of system (1). According to Fig. 6, the regular set of points shown in the Poincaré maps is an indication of system chaotic behavior.

2.3. Problem Formulation of Finite-Time Fast Synchronization

In this section, fast synchronization and its theorems are presented between two new and overly hyperchaotic systems with indefinite parameters and uncertain disturbances. At this point, we use the system of Equation (1) by modifying the initial conditions and its parameters, both master and slave systems for fast synchronization. Consider the hyperchaotic system which refers to the master system.

$$\dot{x}_{im}(\tau) = \begin{bmatrix} -a_{1m} & a_{1m} - a_{4m}x_{3m} & -a_{3m}x_{3m} & -a_{2m} \\ -a_{1m}x_{1m} - a_{8m}x_{2m} & -x_{1m}x_{3m} + a_{5m} & -a_{7m} & -a_{6m} \\ a_{1m}x_{1m} & x_{1m}x_{3m} & -a_{2m} & 0 \\ -a_{11m} + a_{8m}x_{2m} & a_{10m}x_{3m}x_{4m} & a_{9m} + a_{7m}x_{1m}x_{2m} & a_{12m}x_{1m}x_{3m} \end{bmatrix} x_{im} \quad (6)$$

The basic parameters and initial conditions of the master system (6) are defined as follows:

$$\begin{aligned} a_{1m} &= 15, a_{2m} = 4, a_{3m} = 16, a_{4m} = 8, a_{5m} = 0.25, a_{6m} = 23, \\ a_{7m} &= 10, a_{8m} = 3, a_{9m} = 8.12, a_{10m} = 5, a_{11m} = 13, a_{12m} = 20 \\ x_{1m}(0) &= 2.2, x_{2m}(0) = -0.4, x_{3m}(0) = -10, x_{4m}(0) = 1.1 \end{aligned} \tag{7}$$

where $X_m = x_{1m}, \dots, x_{4m}$, $x_{1m}(0), \dots, x_{4m}(0)$ and a_{1m}, \dots, a_{12m} are the states, initial

conditions and parameters of the system (6), respectively. Similarly, for the slave hyperchaotic system, we will have:

$$\dot{x}_{is}(\tau) = \begin{bmatrix} -a_{1s} & a_{1s} - a_{4s}X_{3s} & -a_{3s}X_{3s} & -a_{2s} \\ -a_{1s}X_{1s} - a_{8s}X_{2s} & -X_{1s}X_{3s} + a_{5s} & -a_{7s} & -a_{6s} \\ a_{1s}X_{1s} & X_{1s}X_{3s} & -a_{2s} & 0 \\ -a_{11s} + a_{8s}X_{2s} & a_{10s}X_{3s}X_{4s} & a_{9s} + a_{7s}X_{1s}X_{2s} & a_{12s}X_{1s}X_{3s} \end{bmatrix} x_{is} \tag{8}$$

$+ \Lambda u(\tau) + d(\tau)$ (for $i=1, \dots, 4$)

where $X_s = x_{1s}, \dots, x_{4s}$ are the state variables of the system (8) and $u(\tau) = u_1, \dots, u_4$ are nonlinear command signals which are used to synchronize two systems in equation (6) and equation (8) respectively. The basic parameters and initial conditions of the master system (8) are defined as follows:

$$\begin{aligned} a_{1s} &= 14.9, a_{2s} = 3.85, a_{3s} = 16.19, \\ a_{4s} &= 8.2, a_{5s} = 0.253, a_{6s} = 22.89, \\ a_{7s} &= 9.962, a_{8s} = 3.21, a_{9s} = 7.799, \\ a_{10s} &= 5.05, a_{11s} = 12.92, a_{12s} = 19.75 \\ x_{1s}(0) &= 2.2, x_{2s}(0) = 0.5, \\ x_{3s}(0) &= -9, x_{4s}(0) = 1 \end{aligned} \tag{9}$$

where $x_{1s}(0), \dots, x_{4s}(0)$ and a_{1s}, \dots, a_{12s} are the initial conditions and parameters of the slave system (6), respectively.

Assumption 1: Let denote the synchronization and fast synchronization errors of the system (6) and system (8) as:

$$e_i = x_{is} - x_{im} \quad (i=1, \dots, 4)$$

Assumption 2: In general, consider the constraints on the disturbance and uncertainty as:

$$|f(x(\tau))| \leq \alpha_1, |d(\tau)| \leq \alpha_2 \tag{10}$$

where α_1 and α_2 are positive unknown constants.

Assumption 3: Suppose $y_i(\tau) = x_i(\tau)$ implies that $\lim_{\tau \rightarrow \infty} e_i(\tau) = 0$.

Definition 1 [48]: The systems (6) and (8) can be synchronized in a finite-time if $\lim_{\tau \rightarrow T} \|error(\tau)\| = 0$ and $\|error(\tau)\| = 0$ if $\tau \geq T$, where $T = T(error(0)) > 0$, $error(\tau) = [error_i]^T, (i = 1, \dots, 4)$.

Definition 2 [49]: Master and slave systems (6) and (8) are finite-time synchronized, if there is a controller $v_p(\tau)$ and a constant $T > 0$ such that

$\lim_{\tau \rightarrow T} [Z_p^*(\tau) - Z_p^{**}(\tau)] = 0$, where
 $Z_p^*(\tau) - Z_p^{**}(\tau)$ for $\tau > T$, $Z^*(\tau)$ and $Z^{**}(\tau)$
 are the solutions of master–slave systems (6)
 and (8).

Lemma 1 [50]: If $\mathcal{G}(\tau)$ is a definite and positive performance such that:

$$\dot{\mathcal{G}}(t) \leq -\delta \mathcal{G}^\theta(t), \quad \forall \tau \geq \tau_0, \quad \mathcal{G}(\tau_0) \geq 0 \quad (6)$$

where $\delta > 0$, $0 < \theta < 1$ are known and constants, for any initial time τ_0 . Then function $\mathcal{G}(t)$ satisfies

$$\mathcal{G}^{1-\theta}(\tau) \leq \mathcal{G}^{1-\theta}(\tau_0) - \delta(1-\theta)(\tau - \tau_0), \quad (7)$$

$$\tau_0 \leq \tau \leq \tau_1$$

And

$$\mathcal{G}(\tau) \equiv 0, \quad \forall \tau \geq \tau_1 \quad (8)$$

with the settling time τ_1 satisfying

$$\tau_1 \leq \tau_0 + \frac{\mathcal{G}^{1-\theta}(\tau_0)}{\delta(1-\theta)} \quad (9)$$

Lemma 2: Suppose that the $v(\tau)$ function, which is positive–definite and continuous, satisfies the differential inequality of [51]:

$$\dot{v}(\tau) \leq -\alpha v(\tau) - \beta v^\eta(\tau) \quad (10)$$

$$\forall \tau \geq \tau_0, \quad v(\tau_0) \geq 0$$

for all times τ_0 , the function $v(\tau)$ in the finite time τ_s , will converge to zero. Thus:

$$\tau_s = \tau_0 + \frac{1}{\alpha(1-\eta)} \ln \frac{\alpha v^{1-\eta}(\tau_0) + \beta}{\beta} \quad (11)$$

3. FTSM CONTROLLER

To obtain the finite time tracking approach, the FTSMC surface is

$$s(t) = k_p e(\tau) + k_i \int_0^\tau e(t)^{q/p} dt + k_d \dot{e}(\tau) \quad (12)$$

where k_p, k_i, k_d indicate the positive coefficients, q and p denote the odd positive integer values which $q < p$. Once tracking error $e(\tau)$ reaches the finite-time terminal sliding mode surface $s(\tau) = 0$, we have:

$$k_p e(\tau) + k_i \int_0^\tau e(t)^{q/p} dt + k_d \dot{e}(\tau) = 0 \quad (13)$$

And also $\dot{s}(\tau) = 0$ is produced, which gives

$$\ddot{e}(\tau) = -\frac{k_p}{k_d} \dot{e}(\tau) - \frac{k_i}{k_d} e(\tau)^{q/p} \quad (14)$$

Construct the Lyapunov function by

$$V_0(t) = 0.5 \dot{e}(t)^T \dot{e}(t) + \frac{k_{ip}}{k_d(q+p)} e(t)^T e(t)^{q/p} \quad (15)$$

Taking time-derivative of V_0 and using (14), one finds

$$\begin{aligned} V_0(t) &= \dot{e}(\tau)^T \ddot{e}(\tau) + \frac{k_{ip}}{k_d(q+p)} \left(\frac{q}{p} + 1\right) \dot{e}(\tau)^T e(\tau)^{q/p} \\ &= \dot{e}(\tau)^T \left(-\frac{k_p}{k_d} \dot{e}(\tau) - \frac{k_i}{k_d} e(\tau)^{q/p}\right) + \frac{k_i}{k_d} \dot{e}(\tau)^T e(\tau)^{q/p} \\ &= -\frac{k_p}{k_d} \dot{e}(\tau)^T \dot{e}(\tau) \leq 0 \end{aligned} \quad (16)$$

It means that once the error reaches the finite-time terminal sliding surface (12), the error trajectories converge to the origin asymptotically. In fact, the error trajectories are uniformly bounded. Since the Lyapunov functional is positive definite and its derivative (16) is negative semi-definite, it is resulted in that $\lim_{\tau \rightarrow \infty} V_0(\tau) = V(\infty)$ exists for $V_0(\infty) \in \mathfrak{R}^+$. Based on the boundedness of error states, the term $\dot{V}_0(\tau)$ is a uniformly continuous term. Hence, via Barbalat's lemma, one has $\lim_{\tau \rightarrow \infty} \dot{e}(\tau) = 0$. From (12), the condition $\lim_{\tau \rightarrow \infty} e(\tau) = 0$ obtained. Totally, the error trajectories asymptotically converge to the origin.

Theorem 1: Consider the nonlinear system as

$$\dot{x}(\tau) = a(\tau, x) + b(\tau, x)u(\tau) + d(\tau) \quad (17)$$

The finite-time terminal sliding surface (12) is considered. Using the terminal sliding mode tracker as

$$\begin{aligned} \dot{u}(\tau) = & -\frac{1}{k_d}b(\tau, x) + k_i e(\tau)^{q/p} \\ & + k_p(a(\tau, x)) + k_d(\dot{a}(\tau, x) - \ddot{x}_d(\tau)) \\ & + (k_p b(\tau, x) + k_d \dot{b}(\tau, x))u(\tau) \\ & + \mathcal{G} \operatorname{sgn}(s(\tau)) + \beta_1 |s(\tau)| \operatorname{sgn}(s) \\ & + \beta_2 |s(\tau)|^\alpha \operatorname{sgn}(s) \end{aligned} \quad (18)$$

where $b^+ = b^T (bb^T)^{-1}$ and $\mathcal{G} > \|k_p d(\tau) + k_d \dot{d}(\tau)\|$, then, the designed sliding surface is obliged to converge to the equilibrium in finite-time.

Proof: Using (17) in time-derivative of the sliding surface (12). One has

$$\begin{aligned} \dot{s}(\tau) = & k_p \dot{e}(\tau) + k_i e(\tau)^{q/p} + k_d \dot{e}(\tau) \\ = & k_p (a(\tau, x) + b(\tau, x)u(\tau) \\ & + d(\tau) - \dot{x}_d(\tau)) + k_i e(\tau)^{q/p} \\ & + k_d (\dot{a}(\tau, x) + \dot{b}(\tau, x)u(\tau) \\ & + b(\tau, x)\dot{u}(\tau) + \dot{d}(\tau) - \ddot{x}_d(\tau)) \end{aligned} \quad (19)$$

The Lyapunov function is considered as

$$V_1(\tau) = \frac{1}{2} s(\tau)^T s(\tau) \quad (20)$$

taking time derivative (20) of and by using (19), one attains

$$\begin{aligned} \dot{V}_1(\tau) = & s(\tau)^T \{k_i e(\tau)^{q/p} \\ & + k_p (a(\tau, x) - \dot{x}_d(\tau)) \\ & + k_d (\dot{a}(\tau, x) - \ddot{x}_d(\tau)) \\ & + (k_p b(\tau, x) + k_d \dot{b}(\tau, x))u(\tau) \\ & + k_p d(\tau) + k_d \dot{d}(\tau) \\ & + k_d b(\tau, x)\dot{u}(\tau)\} \end{aligned} \quad (21)$$

Now, substituting (18) into (21), one achieves

$$\begin{aligned} \dot{V}_1(\tau) = & s(\tau)^T \{k_p d(\tau) + k_d \dot{d}(\tau) \\ & - \mathcal{G} \operatorname{sgn}(s(\tau)) - \beta_1 |s(\tau)| \operatorname{sgn}(s) \\ & - \beta_2 |s(\tau)|^\alpha \operatorname{sgn}(s)\} \\ \leq & (\|k_p d(\tau) + k_d \dot{d}(\tau)\| - \mathcal{G}) \|s(\tau)\| \\ & - \beta_1 \|s(\tau)\|^2 - \beta_2 \|s(\tau)\|^{1+\alpha} \\ \leq & \beta_1 \|s(\tau)\|^2 - \beta_2 \|s(\tau)\|^{1+\alpha} < 0 \end{aligned} \quad (22)$$

Since $s(\tau)^T s(\tau) = \|s(\tau)\|^2$, then one can obtain from (20) that $\|s(\tau)\| = \sqrt{2}V_1(\tau)^{0.5}$. Hence, from (22) we have:

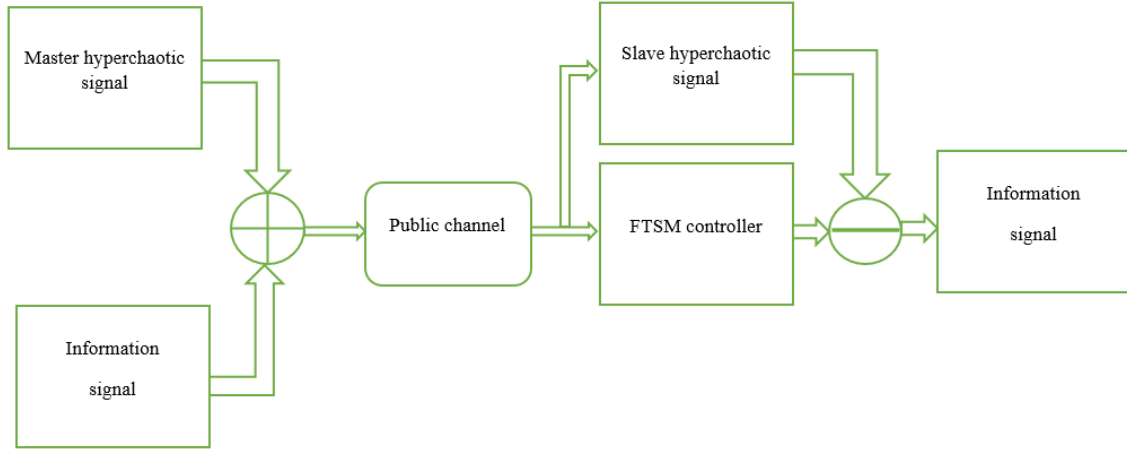


Fig. 7. Block diagram of hyperchaotic communication scheme.

$$V'_1(\tau) \leq -2\beta_1 V_1(\tau) - 2^{\frac{1+\alpha}{2}} \beta_2 V_1(\tau)^{\frac{1+\alpha}{2}} \quad (23)$$

Since the Lyapunov function time-derivative is negative definite, then, the Lyapunov function (20) gradually decreases and sliding surface $s(\tau)$ is convergent to zero in finite-time.

4. HYPERCHAOTIC SYNCHRONIZATION

In this section, we perform the finite-time synchronization between two 4D hyperchaotic systems with unknown disturbances and parametric uncertainty in the system. Here, we used both system (6) and system (8) for the synchronization. It is worth noting that although systems (6) and (8) are the same, for their simulation during synchronization, we consider unequal

parameters and different initial conditions.

Chaotic communication systems have two hyperchaotic systems, the master and slave hyperchaotic systems, and both of them must be synchronized for chaotic communication. In the chaotic communication method, the information signal is added to the chaotic signal at the master. In the slave, the signal received from the public channel is removed from the chaotic signal that is generated by the slave chaotic system. The synchronization error between the state variable of the master and slave chaotic systems is applied to the FTSM controller to produce the control signal. The block diagram of the proposed scheme is shown in Fig. 7.

Based on **Assumption 1**, to study chaos synchronization, the error according to systems (6) and (8), can be designed as follows:

$$e_i = \sum_{i=1}^4 y_i - x_i \Rightarrow \begin{bmatrix} \dot{e}_1 \\ \dot{e}_2 \\ \dot{e}_3 \\ \dot{e}_4 \end{bmatrix} = \begin{bmatrix} -a_1 e_1 + a_1 e_2 - a_2 e_4 + f_1(\tau) \\ a_5 e_2 + a_6 e_4 + f_2(\tau) \\ -a_2 e_3 + f_3(\tau) \\ -a_{11} e_1 + a_9 e_3 + f_4(\tau) \end{bmatrix} + B(\tau)u(\tau) + D(\tau) \quad (24)$$

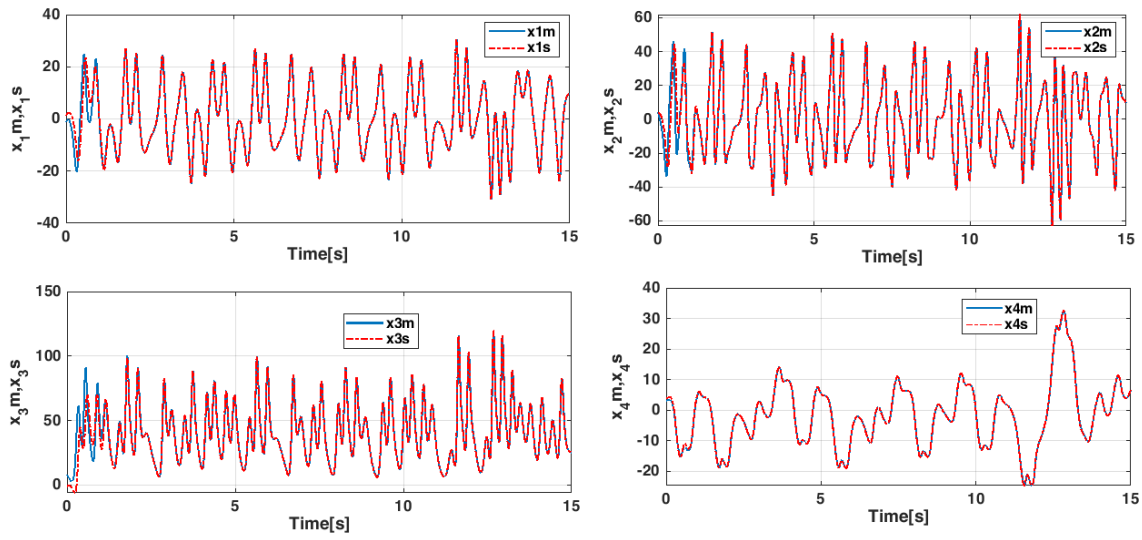


Fig. 8. Synchronization between two states x_{im}, x_{is} for $i = 1, \dots, 4$.

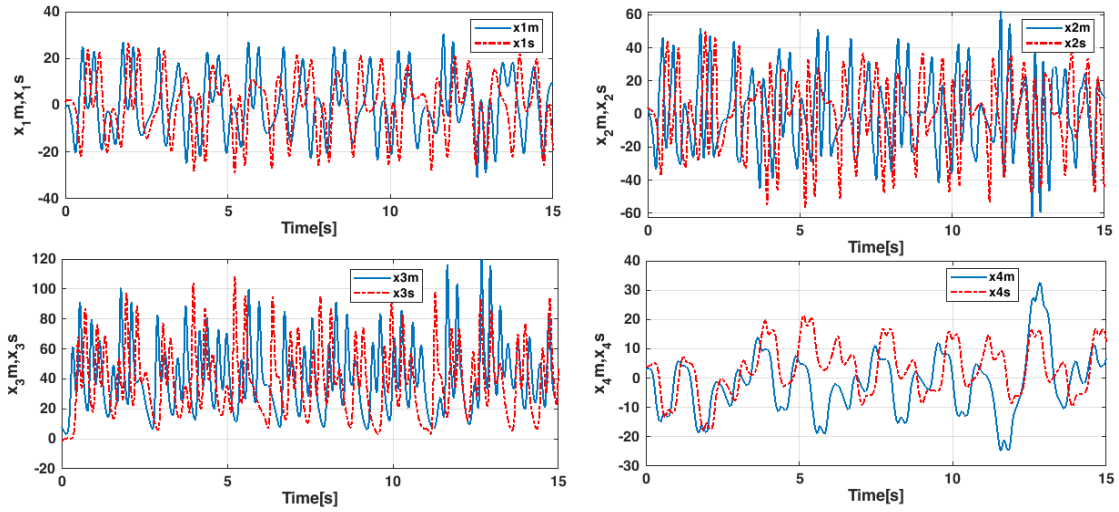


Fig. 9. The errors of synchronization without the controller.

where

$$\begin{aligned}
 f_1(\tau) &= a_{3m}x_{3m}^2 + a_{4m}x_{2m}x_{3m} - a_{3s}x_{3s}^2 - a_{4s}x_{2s}x_{3s}, \\
 f_2(\tau) &= a_{1m}x_{1m}^2 + a_{7m}x_{2m}x_{3m} + a_{8m}x_{1m}x_{2m} + x_{1m}x_{2m}x_{3m} \\
 &\quad - a_{1s}x_{1s}^2 - a_{7s}x_{2s}x_{3s} - a_{8s}x_{1s}x_{2s} - x_{1s}x_{2s}x_{3s}, \\
 f_3(\tau) &= -a_{10m}x_{1m}^2 - x_{1m}x_{2m}x_{3m} + a_{10s}x_{1s}^2 + x_{1s}x_{2s}x_{3s}, \\
 f_4(\tau) &= -a_{7m}x_{1m}x_{2m}x_{3m} - a_{8m}x_{1m}x_{2m} - a_{10m}x_{2m}x_{3m}x_{4m} - a_{12m}x_{1m}x_{3m}x_{4m} \\
 &\quad + a_{7s}x_{1s}x_{2s}x_{3s} + a_{8s}x_{1s}x_{2s} + a_{10s}x_{2s}x_{3s}x_{4s} + a_{12s}x_{1s}x_{3s}x_{4s}
 \end{aligned} \tag{25}$$

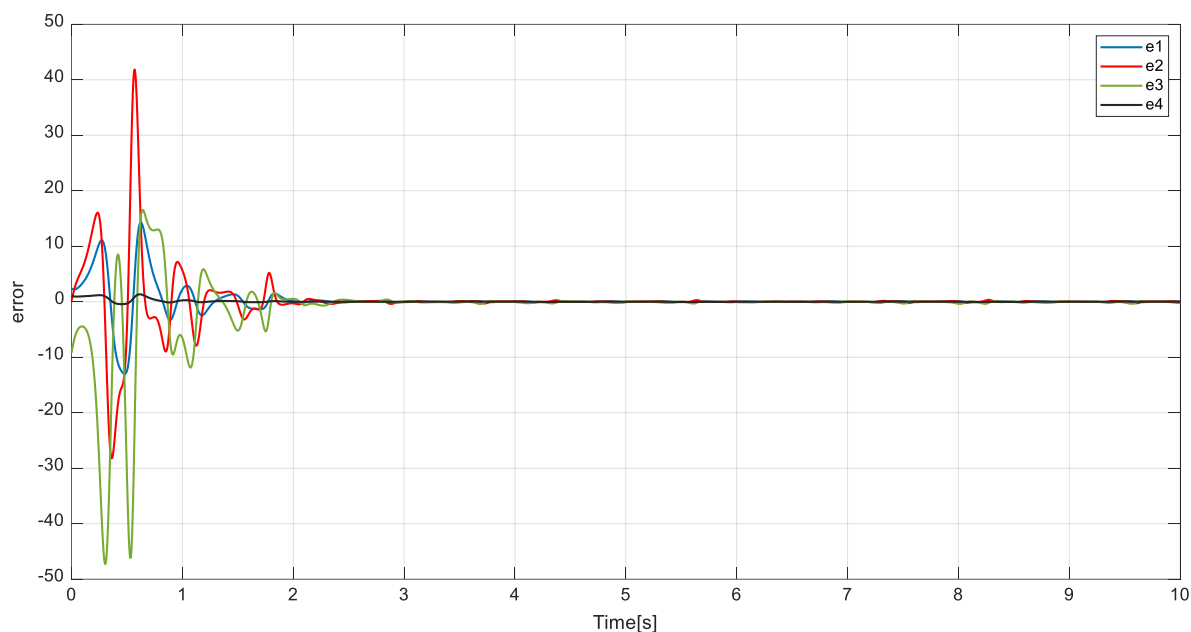


Fig. 10. The errors of synchronization with the controller.

System (24) in the matrix is formed as:

$$\begin{aligned} \frac{de_i(\tau)}{d\tau} = & \Lambda e_i(\tau) + f(e(\tau)) \\ & + B(\tau)u(\tau) + D(\tau) \end{aligned} \quad (26)$$

The control law (18) with $k_p = 600, k_i = 300, k_d = 0.5, \beta_1 = \beta_2 = 25, \vartheta = 10, p = 5, q = 3, \alpha = 0.4$ is designed so that the finite-time synchronization of unknown hyperchaotic systems is performed. Fig. 8 shows the complete hyperchaotic synchronization of the system (6) and (8). According to the equation (18) in the initial conditions, the errors of synchronization without the controller are shown in Fig. 9. When the controller is activated, the errors of synchronization are as in Fig. 10. According to the simulation results, it is easy to see that the master and slave systems are synchronized in finite-time.

5. CONCLUSIONS

In this paper, a novel 4D hyperchaotic system is reported. The dynamic behavior of the proposed system was analyzed using phase portraits, Lyapunov exponent, Poincare map, Kaplan–Yorke dimension, and bifurcation diagram. The new hyperchaotic system has extremely complicated dynamics and structure. Next, one terminal sliding mode controller has been designed for stabilizing the new hyperchaotic system with uncertainty and unknown disturbances. The results obtained from FTSMC were verified using Lyapunov stability theory. A new controller is designed for finite-time synchronization between two identical proposed hyperchaotic systems in the presence of unequal parameters, different initial conditions and matched disturbances are considered for transferring industrial automation information. The new controller feature is that the sliding surface designed

with high-order power function of error and derivative of error was new and stable. The new terminal sliding surface can supply a particular convergence characteristic. Finally, the numerical simulations show the viability of the designed methods. The simulations show that the analytical results and computational are similar.

REFERENCES

- [1] Vaseghi, B., M.A. Pourmina, and S. Mobayen, Secure communication in wireless sensor networks based on chaos synchronization using adaptive sliding mode control. *Nonlinear Dynamics*, 2017. 89(3): p. 1689-1704.
- [2] Scholl, G., et al. Wireless Automation. in 16th International Conference On Sensors and Measurement Technology. 2013.
- [3] Palanisamy, S., S.S. Kumar, and J.L. Narayanan. Secured wireless communication for industrial automation and control. in 2011 3rd International Conference on Electronics Computer Technology. 2011. IEEE.
- [4] Neumann, P., Communication in industrial automation—What is going on? *Control Engineering Practice*, 2007. 15(11): p. 1332-1347.
- [5] Sheela, S., K. Suresh, and D. Tandur. Security of industrial wireless sensor networks: a review. in 2015 International Conference on Trends in Automation, Communications and Computing Technology (I-TACT-15). 2015. IEEE.
- [6] Christin, D., P.S. Mogre, and M. Hollick, Survey on wireless sensor network technologies for industrial automation: The security and quality of service perspectives. *Future Internet*, 2010. 2(2): p. 96-125.
- [7] Zhang, Z., et al., Privacy-enhanced momentum federated learning via differential privacy and chaotic system in industrial Cyber-Physical systems. *ISA transactions*, 2021.
- [8] Pai, M.C., Chaos control of uncertain time-delay chaotic systems with input dead-zone nonlinearity. *Complexity*, 2016. 21(3): p. 13-20.
- [9] Wang, X., N.V. Kuznetsov, and G. Chen, Chaotic systems with multistability and hidden attractors. 2021: Springer.
- [10] Xian, Y. and X. Wang, Fractal sorting matrix and its application on chaotic image encryption. *Information Sciences*, 2021. 547: p. 1154-1169.
- [11] Moysis, L., et al., Analysis, synchronization, and robotic application of a modified hyperjerk chaotic system. *Complexity*, 2020. 2020.
- [12] Lin, H., et al., Chaotic dynamics in a neural network with different types of external stimuli. *Communications in Nonlinear Science and Numerical Simulation*, 2020. 90: p. 105390.
- [13] Ribera, H., et al., Model selection of chaotic systems from data with hidden variables using sparse data assimilation. *arXiv preprint arXiv:2105.10068*, 2021.
- [14] Chen, Y.-J., et al., A polynomial-fuzzy-model-based synchronization methodology for the multi-scroll Chen chaotic secure communication system.

- Engineering Applications of Artificial Intelligence, 2020. 87: p. 103251.
- [15] Zhang, S. and T. Gao, A coding and substitution frame based on hyperchaotic systems for secure communication. *Nonlinear Dynamics*, 2016. 84(2): p. 833-849.
- [16] Chen, G. and T. Ueta, Yet another chaotic attractor. *International Journal of Bifurcation and chaos*, 1999. 9(07): p. 1465-1466.
- [17] Lü, J. and G. Chen, A new chaotic attractor coined. *International Journal of Bifurcation and chaos*, 2002. 12(03): p. 659-661.
- [18] Qi, G., et al., Analysis of a new chaotic system. *Physica A: Statistical Mechanics and its Applications*, 2005. 352(2-4): p. 295-308.
- [19] Rossler, O., An equation for hyperchaos. *Physics Letters A*, 1979. 71(2-3): p. 155-157.
- [20] Dimassi, H. and A. Loría, Adaptive unknown-input observers-based synchronization of chaotic systems for telecommunication. *IEEE Transactions on Circuits and Systems I: Regular Papers*, 2010. 58(4): p. 800-812.
- [21] Al-sawalha, M.M. and A.F. Al-Dababseh, Nonlinear Anti-Synchronization of Two Hyper chaotic Systems. *Applied Mathematical Sciences*, 2011. 5(38): p. 1849-1856.
- [22] Jalnine, A.Y., Generalized synchronization of identical chaotic systems on the route from an independent dynamics to the complete synchrony. *Regular and Chaotic Dynamics*, 2013. 18(3): p. 214-225.
- [23] Gonchenko, A.S., S.V. Gonchenko, and A.O. Kazakov, Richness of chaotic dynamics in nonholonomic models of a Celtic stone. *Regular and Chaotic Dynamics*, 2013. 18(5): p. 521-538.
- [24] Barhaghtalab, M.H., S. Mobayen, and F. Merrikh-Bavat. Design of a Global Sliding Mode Controller Using Hyperbolic Functions for Nonlinear Systems and Application in Chaotic Systems. in 2019 27th Iranian Conference on Electrical Engineering (ICEE). 2019. IEEE.
- [25] Wu, X., C. Zhu, and H. Kan, An improved secure communication scheme based passive synchronization of hyperchaotic complex nonlinear system. *Applied Mathematics and Computation*, 2015. 252: p. 201-214.
- [26] Singh, P.P., J.P. Singh, and B. Roy. Tracking control and synchronization of Bhalekar-Gejji chaotic systems using active backstepping control. in 2018 IEEE International Conference on Industrial Technology (ICIT). 2018. IEEE.
- [27] Henein, M.M., et al. Switched active control synchronization of three fractional order chaotic systems. in 2016 13th International Conference on Electrical Engineering/Electronics, Computer, Telecommunications and Information Technology (ECTI-CON). 2016. IEEE.
- [28] Liu, Z., Design of nonlinear optimal control for chaotic synchronization of coupled stochastic neural networks via Hamilton–Jacobi–Bellman equation. *Neural Networks*, 2018. 99: p. 166-177.
- [29] Mobayen, S. and S. Javadi, Disturbance observer and finite-time tracker design

- of disturbed third-order nonholonomic systems using terminal sliding mode. *Journal of Vibration and Control*, 2017. 23(2): p. 181-189.
- [30] Pisano, A. and E. Usai, Output-feedback control of an underwater vehicle prototype by higher-order sliding modes. *Automatica*, 2004. 40(9): p. 1525-1531.
- [31] Besnard, L., Y.B. Shtessel, and B. Landrum, Quadrotor vehicle control via sliding mode controller driven by sliding mode disturbance observer. *Journal of the Franklin Institute*, 2012. 349(2): p. 658-684.
- [32] Konishi, K., M. Hirai, and H. Kokame, Sliding mode control for a class of chaotic systems. *Physics letters A*, 1998. 245(6): p. 511-517.
- [33] Yau, H.-T., C.o.-K. Chen, and C.-L. Chen, Sliding mode control of chaotic systems with uncertainties. *International Journal of Bifurcation and Chaos*, 2000. 10(05): p. 1139-1147.
- [34] Li, H., et al., Chaos control and synchronization via a novel chatter free sliding mode control strategy. *Neurocomputing*, 2011. 74(17): p. 3212-3222.
- [35] Mobayen, S., An adaptive chattering-free PID sliding mode control based on dynamic sliding manifolds for a class of uncertain nonlinear systems. *Nonlinear Dynamics*, 2015. 82(1-2): p. 53-60.
- [36] Xi, X., et al., Robust finite-time synchronization of a class of chaotic systems via adaptive global sliding mode control. *Journal of Vibration and Control*, 2018. 24(17): p. 3842-3854.
- [37] Zirkohi, M.M., An efficient approach for digital secure communication using adaptive backstepping fast terminal sliding mode control. *Computers & Electrical Engineering*, 2019. 76: p. 311-322.
- [38] Yang, Y., et al., Dynamical analysis and image encryption application of a novel memristive hyperchaotic system. *Optics & Laser Technology*, 2021. 133: p. 106553.
- [39] Yu, F., et al., A new 4D four-wing memristive hyperchaotic system: dynamical analysis, electronic circuit design, shape synchronization and secure communication. *International Journal of Bifurcation and Chaos*, 2020. 30(10): p. 2050147.
- [40] Mostafaei, J., et al., Complex dynamical behaviors of a novel exponential hyper-chaotic system and its application in fast synchronization and color image encryption. *Science Progress*, 2021. 104(1): p. 00368504211003388.
- [41] Wiggins, S., Introduction to applied nonlinear dynamical systems and chaos. Vol. 2. 2003: Springer Science & Business Media.
- [42] Zhang, X., H. Zhu, and H. Yao, Analysis of a new three-dimensional chaotic system. *Nonlinear Dynamics*, 2012. 67(1): p. 335-343.
- [43] Wolf, A., et al., Determining Lyapunov exponents from a time series. *Physica D: Nonlinear Phenomena*, 1985. 16(3): p. 285-317.
- [44] Li, C., et al., On the bound of the Lyapunov exponents for the fractional differential systems. *Chaos: An Interdisciplinary Journal of Nonlinear*

- Science, 2010. 20(1): p. 013127.
- [45] Frederickson, P., et al., The Liapunov dimension of strange attractors. *Journal of differential equations*, 1983. 49(2): p. 185-207.
- [46] Mahmoud, E.E., Generation and suppression of a new hyperchaotic nonlinear model with complex variables. *Applied Mathematical Modelling*, 2014. 38(17-18): p. 4445-4459.
- [47] Mahmoud, E.E., Dynamics and synchronization of new hyperchaotic complex Lorenz system. *Mathematical and Computer Modelling*, 2012. 55(7-8): p. 1951-1962.
- [48] Yang, X. and J. Cao, Finite-time stochastic synchronization of complex networks. *Applied Mathematical Modelling*, 2010. 34(11): p. 3631-3641.
- [49] Abdurahman, A., H. Jiang, and Z. Teng, Finite-time synchronization for memristor-based neural networks with time-varying delays. *Neural Networks*, 2015. 69: p. 20-28.
- [50] Bao, H. and J. Cao, Finite-time generalized synchronization of nonidentical delayed chaotic systems. *Nonlinear Analysis: Modelling and Control*, 2016. 21(3): p. 306-324.
- [51] Moulay, E. and W. Perruquetti, Finite time stability and stabilization of a class of continuous systems. *Journal of Mathematical analysis and applications*, 2006. 323(2): p. 1430-1443.